

## Formation of $\beta$ - and $\beta''$ - $\text{Al}_2\text{O}_3$ by the Solid State Reaction between $\text{NaAlO}_2$ and $\gamma$ - $\text{Al}_2\text{O}_3$

TAKEHIKO TAKAHASHI AND KATSUMI KUWABARA

*Department of Applied Chemistry, Faculty of Engineering, Nagoya University, Nagoya 464, Japan*

Received October 10, 1978; in revised form January 31, 1979

The solid state reaction of  $\text{NaAlO}_2$  with  $\gamma$ - $\text{Al}_2\text{O}_3$  was investigated kinetically. Powdered compacts with various compositions ( $\text{Al}_2\text{O}_3/\text{NaAlO}_2 = 1-5$ ) were fired at 700–1200°C for 1–768 hr. The amounts of the reaction product were determined by peak heights of X-ray diffraction patterns.  $\beta''$ - $\text{Al}_2\text{O}_3$  was formed predominantly from the sample with  $\text{Al}_2\text{O}_3/\text{NaAlO}_2 = 2$ . The firing time for the  $\beta''$ - $\text{Al}_2\text{O}_3$  formation was shortened as the firing temperature was raised, and the activation energy,  $E_a$ , for formation was about 130–135 kcal/mole. The sample of  $\text{Al}_2\text{O}_3/\text{NaAlO}_2 = 5$  formed *m*- $\text{Al}_2\text{O}_3$  with the mullite structure and was observed to transform gradually to  $\beta$ - $\text{Al}_2\text{O}_3$ .  $E_a$  for the *m*- $\text{Al}_2\text{O}_3$  formation and for the transition were about 55–60 and 40 kcal/mole, respectively, which resulted in  $E_a$  of about 95–100 kcal/mole for the  $\beta$ - $\text{Al}_2\text{O}_3$  formation. The mechanism of the *m*- $\text{Al}_2\text{O}_3$  formation is discussed briefly.

### Introduction

$\beta$ -Alumina ( $\beta$ - $\text{Al}_2\text{O}_3$ ) is the most representative sodium ion conductor, and is used as the solid electrolyte for the sodium-sulfur battery. Many studies have been done to define the phase relations in the system  $\text{NaAlO}_2$ - $\text{Al}_2\text{O}_3$  (1–3) in the temperature region above 1100°C, since highly conductive and dense ceramics of  $\beta$ - $\text{Al}_2\text{O}_3$  are obtained only by high-temperature firing or high-temperature-pressure treatment.

Recently, Perrotta and Young (4) found a mullite-type phase called "*m*- $\text{Al}_2\text{O}_3$ " below 1000°C by a gel crystallization technique. Elliot and Huggins (5) confirmed a phase, designated " $\lambda$ ," below 1100°C by ashing filter paper soaked in aqueous salt solutions. The " $\lambda$ - $\text{Al}_2\text{O}_3$ " which has the composition  $\text{Na}_2\text{O} \cdot n\text{Al}_2\text{O}_3$  ( $3 \cong n < 12$ ) appears to be the same phase as *m*- $\text{Al}_2\text{O}_3$ . These workers pointed out that formation of this phase

depended on very intimate and uniform mixing of reactants on a microscopic level.

The present authors have found that the mullite-type alumina is formed as a result of direct solid state reaction between  $\text{NaAlO}_2$  and  $\gamma$ - $\text{Al}_2\text{O}_3$  below 1100°C and transforms to  $\beta$ - $\text{Al}_2\text{O}_3$ . This paper describes a kinetic study of the  $\beta''$ -, *m*-, and  $\beta$ - $\text{Al}_2\text{O}_3$  formation.

### Experimental

One of the starting materials, sodium aluminate, was prepared by heating commercial sodium aluminate at 200°C for 10 hr in air and dried at 100°C for several hours in a vacuum drier. Another starting material,  $\gamma$ - $\text{Al}_2\text{O}_3$ , was obtained by thermal decomposition of aluminum sulfate at 900°C for 3 hr in flowing nitrogen and dried in the same manner as  $\text{NaAlO}_2$ . Compositions examined in the system  $\text{NaAlO}_2$ - $\text{Al}_2\text{O}_3$  were  $\text{Al}_2\text{O}_3/\text{NaAlO}_2 = 1-5$ . In order to simplify

the description of the composition, the sample of  $\text{Al}_2\text{O}_3/\text{NaAlO}_2 = n$  is written in the form of N- $n$ A, so that  $\text{NaAlO}_2$ :  $\gamma$ - $\text{Al}_2\text{O}_3 = 1:5$ , for example, is indicated as N-5A. The starting materials were weighed, mixed in a ball-mill using ethanol as a dispersing reagent, and dried at  $110^\circ\text{C}$  in the vacuum drier. The mixed powders were found to consist of particles smaller than several micrometers by observation with a scanning electron microscope.

Tablets of 13-mm diameter and 2-mm thickness formed by pressing the powder were heated in air at a certain temperature in the range  $700$ – $1200^\circ\text{C}$  for a scheduled time for an interval of 1–768 hr. The calcined tablets were ground to a fine powder for X-ray diffraction.

In order to determine the amounts of reaction product, the heights of the peaks of the diffraction patterns were measured; the amounts of  $\beta$ -,  $\beta''$ - and  $m$ - $\text{Al}_2\text{O}_3$  cannot be determined chemically since they have almost the same chemical properties. The (004) and (006) reflections were used to determine the contents of  $\beta$ - and  $\beta''$ - $\text{Al}_2\text{O}_3$ , respectively. The (004) reflection for  $\beta$ - $\text{Al}_2\text{O}_3$  has almost the same spacing as the (006) reflection for  $\beta''$ - $\text{Al}_2\text{O}_3$ , so their peaks overlap completely on the diffraction chart. However, in the region rich in  $\text{NaAlO}_2$ , mainly  $\beta''$ - $\text{Al}_2\text{O}_3$  was detected, hence a trace amount of  $\beta$ - $\text{Al}_2\text{O}_3$  could be neglected in this experiment. On the contrary, in the region rich in  $\gamma$ - $\text{Al}_2\text{O}_3$ , predominantly  $\beta$ - $\text{Al}_2\text{O}_3$  was found so that trace amounts of  $\beta''$ - $\text{Al}_2\text{O}_3$  and  $\alpha$ - $\text{Al}_2\text{O}_3$  were neglected.

The (110) and (210) reflections for  $m$ - $\text{Al}_2\text{O}_3$  were useful for the measurement of the heights. The peaks of  $\text{NaAlO}_2$  and  $\gamma$ - $\text{Al}_2\text{O}_3$  were not always available because their intensities were comparatively weak and often overlapped with peaks of other phases. Therefore, calibration curves for  $\gamma$ -,  $\beta$ -,  $\beta''$ -, and  $m$ - $\text{Al}_2\text{O}_3$  were drawn using the (102) reflection for zinc oxide as an internal standard. The content of  $\text{NaAlO}_2$

was ignored to simplify the following discussion.

## Results

### 1. Firing Temperature ( $\theta$ )–Time ( $t$ ) Diagrams

The result of the heat treatment of the sample N-2A is shown in Fig. 1. It indicates that  $\beta''$ - $\text{Al}_2\text{O}_3$  is formed by firing for a shorter time as the temperature rises, and the slope of the curve of  $\theta$  vs  $\log t$  for the appearance of  $\beta''$ - $\text{Al}_2\text{O}_3$  is nearly equal to that for the disappearance of  $\text{NaAlO}_2$ . Figure 2 shows the phase relations of N-5A fired under various conditions. In this figure three curves of  $\theta$  vs  $\log t$  are drawn for the appearance of  $m$ - and  $\beta$ - $\text{Al}_2\text{O}_3$  and for the disappearance of  $m$ - $\text{Al}_2\text{O}_3$ . It can be seen that the slope of the curve for the appearance of  $m$ - $\text{Al}_2\text{O}_3$  is nearly equal to that for the disappearance of the same phase.

The sample N-1A gave a product containing unreacted  $\text{NaAlO}_2$  together with  $\beta''$ - $\text{Al}_2\text{O}_3$  after being fired at high temperatures or treated for a long time even at low temperatures. The products from N-3A and N-4A contained mixed products of N-2A and N-5A.

### 2. Content ( $C$ )–Firing Time ( $t$ ) Curves

The curves of the degree of  $\beta''$ - $\text{Al}_2\text{O}_3$  formation and of  $\gamma$ - $\text{Al}_2\text{O}_3$  consumption in

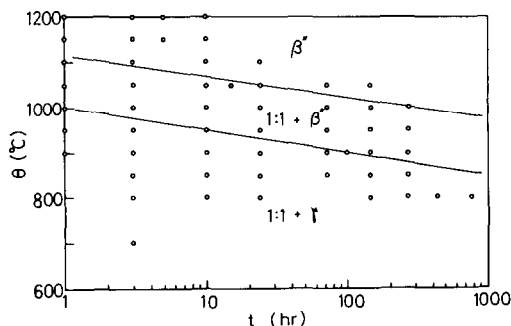


FIG. 1. Reaction products from  $\text{NaAlO}_2$  and  $\gamma$ - $\text{Al}_2\text{O}_3$  (1:2) under various firing conditions shown by open circles.

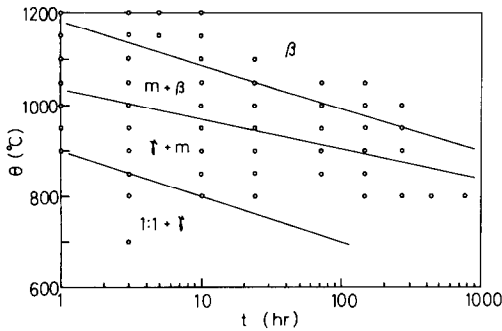


FIG. 2. Reaction products from  $\text{NaAlO}_2$  and  $\gamma\text{-Al}_2\text{O}_3$  (1:5) under various firing conditions shown by open circles.

N-2A are shown in Fig. 3. The content of the  $\beta''$  phase saturates in a shorter time with rising temperature and the value for the  $\gamma$  phase decreases symmetrically as the curve for the  $\beta''$  phase rises. In the case of N-5A,  $m\text{-Al}_2\text{O}_3$  was detected prior to  $\beta\text{-Al}_2\text{O}_3$  and the  $m$  phase disappears gradually as the  $\beta$  phase grows. Figure 4 shows the X-ray diffraction patterns of the specimens fired at  $950^\circ\text{C}$  for various time durations, and the variations in the contents of the three kinds of alumina phases are indicated in Figs. 5, 6, and 7. These figures suggest that the reaction in sample N-5A is a kind of successive reaction.

3. Dependence of Formation Time on Temperature

In the kinetic study of the mullite formation from kaolinite, Lundin (6) proposed the

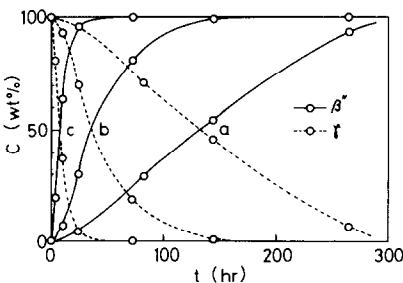


FIG. 3. Variations of  $\beta''$ - and  $\gamma\text{-Al}_2\text{O}_3$  contents in N-2A fired at  $900^\circ\text{C}$  (a),  $950^\circ\text{C}$  (b), and  $1000^\circ\text{C}$  (c).

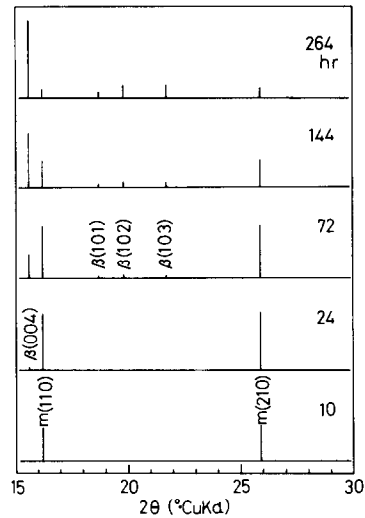


FIG. 4. X-Ray diffraction patterns of the reaction products of N-5A fired at  $950^\circ\text{C}$ .

following experimental equation on the assumption that the rate-determining step is a diffusion process:

$$\log\left(\frac{m_\infty - m}{m_\infty}\right) = \varphi\left(\frac{t}{\theta}\right), \quad (1)$$

where  $m_\infty$  is the mullite content at infinite time ( $t = \infty$ ),  $m$  is the mullite content of the sample at time  $t$ , and  $\theta$  is the characteristic time constant. This  $\theta$  is related to the firing temperature and is given by an Arrhenius equation,

$$\theta = a \cdot \exp(E_a/RT), \quad (2)$$

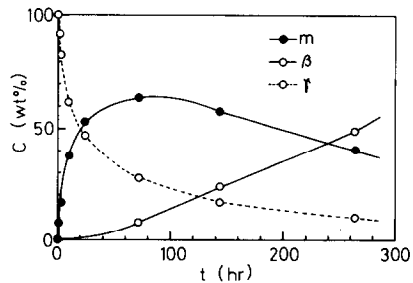


FIG. 5. Variations of contents of  $m$ -,  $\beta$ -, and  $\gamma\text{-Al}_2\text{O}_3$  in N-5A fired at  $900^\circ\text{C}$ .

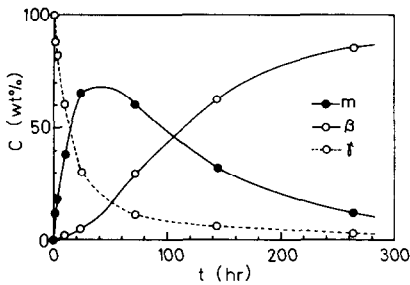


FIG. 6. Variations of contents of  $m$ -,  $\beta$ -, and  $\gamma$ - $\text{Al}_2\text{O}_3$  in N-5A fired at  $950^\circ\text{C}$ .

where  $a$  is a constant and  $E_a$  is the activation energy for the reaction.

In the present work, after modification of the meaning of  $\theta$  as follows, Eq. (2) was applied to several steps in the formation of  $\beta''$ -,  $m$ -, and  $\beta$ - $\text{Al}_2\text{O}_3$ . Figure 8 draws the Lundin plots, where the term "initiation" means the firing time when a phase under consideration is identified initially by the X-ray diffraction pattern, and "maximization" means the firing time when the  $m$  phase has a maximum content. Concerning the  $\beta''$ - and  $\beta$ - $\text{Al}_2\text{O}_3$  formations, the activation energies,  $E_a$ , are calculated to be 135 and 100 kcal/mole from the slopes for the initiation of the phases in N-2A and N-5A, respectively, whereas  $E_a$  for the initiation of the  $m$  phase in N-5A is 60 kcal/mole, which is equal to that for the maximization of the  $m$  phase.

#### 4. Kinetics of $\beta''$ - and $\beta$ - $\text{Al}_2\text{O}_3$ formations

In many solid state reactions and phase transitions, complex nucleation-growth

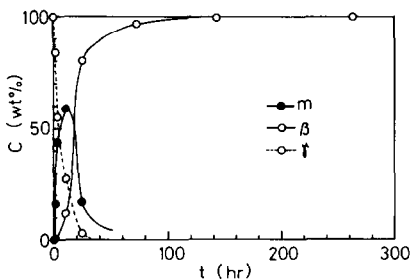


FIG. 7. Variations of contents of  $m$ -,  $\beta$ -, and  $\gamma$ - $\text{Al}_2\text{O}_3$  in N-5A fired at  $1000^\circ\text{C}$ .

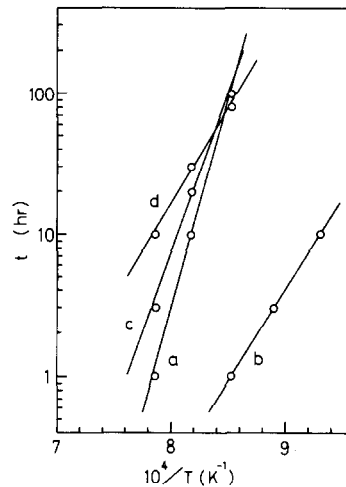


FIG. 8. Lundin plots of initiations of  $\beta''$ - (a),  $m$ - (b), and  $\beta$ - $\text{Al}_2\text{O}_3$  (c) and maximization of  $m$ - $\text{Al}_2\text{O}_3$  (d).

reactions can be seen. When nuclei are formed in the crystal and growing fronts begin to overlap each other, the area of the boundary between the reactant and the product decreases and the reaction rate is slowed down. Nucleation and growth proceed after an induction period, which results in a sigmoid curve for a plot of the content versus firing time. According to Avrami (7) and Erofeev (8), the degree of conversion,  $\alpha$ , of a substance is related to the reaction time,  $t$ , by the following equation,

$$\alpha = 1 - \exp(-Bt^n), \quad (3)$$

where  $B$  and  $n$  are constants.

The formations of  $\beta''$ - and  $\beta$ - $\text{Al}_2\text{O}_3$  in the present study follow sigmoid curves, as seen in Figs. 3, 6, and 7. The substitution of the content of  $\beta''$ - or  $\beta$ - $\text{Al}_2\text{O}_3$ ,  $C$ , for  $\alpha$  in Eq. (3) leads to the conventional relation,

$$\ln[-\ln(1-C)] = \ln B + n \ln t. \quad (4)$$

Figure 9 shows the  $\ln[-\ln(1-C)]$  vs  $\ln t$  plot for the formation of  $\beta''$ - $\text{Al}_2\text{O}_3$  in N-2A. The values taken at a definite temperature fall well on a straight line. The applicability of Eq. (4) was also confirmed for the formation of  $\beta$ - $\text{Al}_2\text{O}_3$  in N-5A. The values of  $B$  were

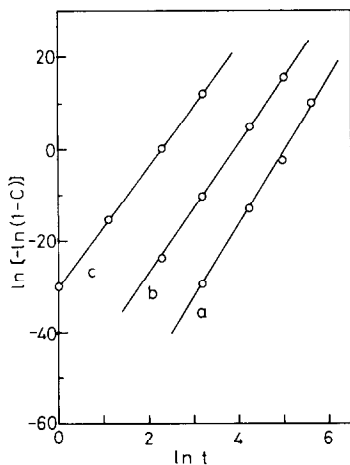


FIG. 9. Avrami-Erofeev plot of  $\beta''$ - $Al_2O_3$  content in N-2A fired at 900°C (a), 950°C (b), and 1000°C (c).

calculated from the values of  $\ln[-\ln(1-C)]$  extrapolated to  $t = 1$ , and these are plotted against the reciprocal of the absolute temperature for two phases in Fig. 10.  $E_a$  are estimated to be about 130 and 95 kcal/mole for  $\beta''$ - and  $\beta$ - $Al_2O_3$ , respectively, which are approximately equal to the values obtained from the Lundin plot.

5. Kinetics of  $m$ - $Al_2O_3$  Formation

Generally, in the investigation of solid state reactions in powdered compacts,

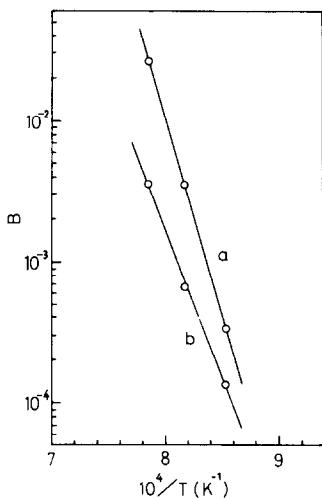


FIG. 10. Dependence of  $B$  in Eq. (4) on temperature for  $\beta''$ - (a) and  $\beta$ - $Al_2O_3$  (b) formations.

several assumptions such as that the reaction is diffusion limited and follows Fick's law are made to simplify the analyses of the kinetics. Jander (9) obtained the well-known relationship

$$[1 - (1-x)^{1/3}]^2 = Kt, \quad (5)$$

where  $x$  is the fraction of an original sphere which has reacted at time  $t$  and  $K$  is a constant related to the diffusion coefficient and to the radius of the sphere.

If an experimental plot of  $x$  vs  $t$  gives the familiar parabolic curve, it will be useful to apply Eq. (5) to the present reaction. As can be seen from Figs. 5, 6, and 7, the plots of  $C$  vs  $t$  for the  $m$ - $Al_2O_3$  formation seem to follow parabolic curves until the fractions of the phase reach the maximum values. Applying the Jander equation to these regions, the values of  $[1 - (1-C)^{1/3}]^2$  are plotted against  $t$ , as shown in Fig. 11. Figure 12 shows the Arrhenius plot of  $K$  together with the similar plot obtained from the Ginstling and Brounshtein equation (10) which is a modified form of the Jander relationship. The apparent activation energies calculated from the slopes of the curves are both about 55 kcal/mole which is almost as large as that obtained from the Lundin plot.

Discussion

1. Stabilities of  $\beta$ -,  $\beta''$ -, and  $m$ - $Al_2O_3$

Several phase diagrams have been reported for the system  $NaAlO_2$ - $Al_2O_3$ . Two

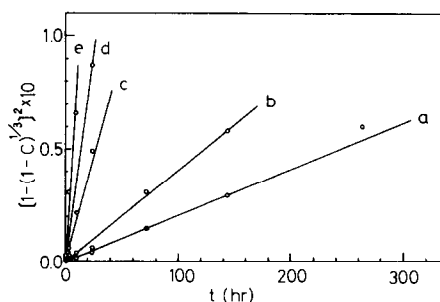


FIG. 11. Jander plot of  $m$ - $Al_2O_3$  content in N-5A fired at 800°C (a), 850°C (b), 900°C (c), 950°C (d), and 1000°C (e).

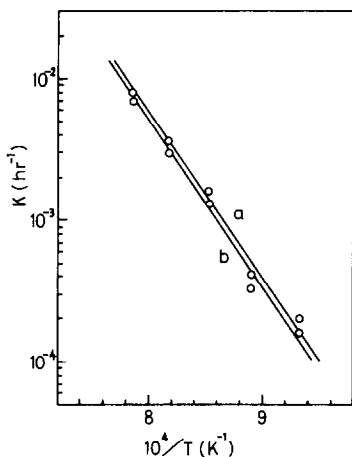


FIG. 12. Temperature dependence of  $K$  in equations by Jander (a) and by Ginstling-Brounshtein (b).

typical diagrams were deduced from a critical evaluation of available data by DeVries and Roth (1). One is for the case where  $\beta$ - $\text{Al}_2\text{O}_3$  is considered to be metastable below about  $1500^\circ\text{C}$  and the other is for the case where  $\beta$ - $\text{Al}_2\text{O}_3$  is stable at all temperatures up to the incongruent melting point. These diagrams, however, lack information below  $1100^\circ\text{C}$ . Liebertz (2) suggested that  $\beta$ - $\text{Al}_2\text{O}_3$  is a metastable phase at that temperature, while Fally *et al.* (3) showed that  $\beta$ - and  $\beta''$ - $\text{Al}_2\text{O}_3$  always coexist at temperatures as low as  $1100^\circ\text{C}$ .

Whether the  $\beta$  phase is stable or not in the range of temperatures lower than  $1100^\circ\text{C}$  can be judged from equilibrium thermodynamic data. Thermodynamic data concerning the Gibbs free energy change of formation of  $\beta$ - $\text{Al}_2\text{O}_3$  were given only in the review (11) in which Weber obtained data electrochemically using a galvanic cell. On the basis of these data, the present authors calculated free energy changes for several reactions with the aid of the JANAF thermodynamic tables. Figure 13 shows the temperature-dependence of the standard free energy changes. Although  $\gamma$ - $\text{Al}_2\text{O}_3$  was used as one of the starting materials in this work, the data for the case where  $\alpha$ - $\text{Al}_2\text{O}_3$  is used as the reactant are also indicated.

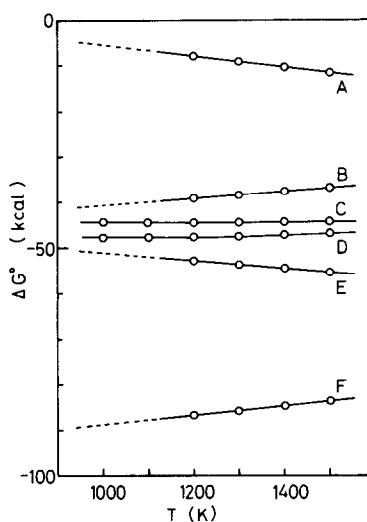


FIG. 13. Standard free energy changes for the reactions: (A)  $2\text{NaAlO}_2 + 10\text{Al}_2\text{O}_3(\alpha) \rightarrow \text{Na}_2\text{O} \cdot 11\text{Al}_2\text{O}_3$ ; (B)  $2\text{NaAlO}_2 + 10\text{Al}_2\text{O}_3(\gamma) \rightarrow \text{Na}_2\text{O} \cdot 11\text{Al}_2\text{O}_3$ ; (C)  $\text{Na}_2\text{O} + \text{Al}_2\text{O}_3(\alpha) \rightarrow 2\text{NaAlO}_2$ ; (D)  $\text{Na}_2\text{O} + \text{Al}_2\text{O}_3(\gamma) \rightarrow 2\text{NaAlO}_2$ ; (E)  $\text{Na}_2\text{O} + 11\text{Al}_2\text{O}_3(\alpha) \rightarrow \text{Na}_2\text{O} \cdot 11\text{Al}_2\text{O}_3$ ; and (F)  $\text{Na}_2\text{O} + 11\text{Al}_2\text{O}_3(\gamma) \rightarrow \text{Na}_2\text{O} \cdot 11\text{Al}_2\text{O}_3$ .

According to this figure, the  $\Delta G^\circ$  values in reactions (A) and (E) increase as temperature decreases, whereas those in reactions (B) and (F) decrease with decreasing temperature. The difference in these behaviors appears to be based on the free energy change of the transition from  $\gamma$ - $\text{Al}_2\text{O}_3$  to  $\alpha$ - $\text{Al}_2\text{O}_3$ . No matter what modification of alumina may be involved, the  $\beta$  phase should be formed and stable thermodynamically even in the temperature region lower than  $1000^\circ\text{C}$ . This was confirmed in the present experiment as can be seen from Fig. 2, though  $\beta$ - $\text{Al}_2\text{O}_3$  was formed very slowly at lower temperatures.

The stabilities of  $\beta''$ - and  $m$ - $\text{Al}_2\text{O}_3$  cannot be judged thermodynamically due to the lack of data for these phases. However, Fig. 1 suggests that  $\beta''$ - $\text{Al}_2\text{O}_3$  is stable at least under the experimental conditions, and it is clear that the  $m$  phase is metastable as shown in Figs. 5, 6, and 7.

## 2. Mechanism of $m\text{-Al}_2\text{O}_3$ Formation

Elliot and Huggins (5) pointed out that mullite-like " $\lambda\text{-Al}_2\text{O}_3$ " is formed only through microscopic mixing of reactants and that absorption of species by filter paper or by mixing with a gel is a convenient technique for achieving the required degree of homogeneity. In the present work, however, the compacts of the mixed powders of  $\text{NaAlO}_2$  and  $\gamma\text{-Al}_2\text{O}_3$  were found to react in the solid state to form  $m\text{-Al}_2\text{O}_3$  with the mullite structure by heating below  $1100^\circ\text{C}$  for an appropriate time. As shown in Fig. 13, the  $\Delta G^\circ$  values for reactions (C) and (D) are almost the same and independent of temperature, so the dissociation reaction  $2\text{NaAlO}_2 \rightarrow \text{Na}_2\text{O} + \text{Al}_2\text{O}_3$  will not proceed and  $\text{NaAlO}_2$  will take part directly in the reaction with  $\gamma\text{-Al}_2\text{O}_3$ .

According to Ghate *et al.* (12), if  $\gamma\text{-Al}_2\text{O}_3$  is in close contact with amorphous silica, the formation of mullite is facilitated by absorption of silica into  $\gamma\text{-Al}_2\text{O}_3$  by the rearrangement of the defect spinel structure. Therefore,  $m\text{-Al}_2\text{O}_3$  with a structure analogous to mullite seems to be formed by the solid state reaction between  $\text{NaAlO}_2$  and  $\gamma\text{-Al}_2\text{O}_3$  with a mechanism similar to that of the reaction in the system  $\text{SiO}_2\text{-}\gamma\text{-Al}_2\text{O}_3$ . After  $\text{NaAlO}_2$  is absorbed into  $\gamma\text{-Al}_2\text{O}_3$ , one of the reactants must diffuse into the particles of the other, though the diffusion species has not been specified.

Though the result that a sample such as N-2A which was rich in  $\text{NaAlO}_2$  in the system  $\text{NaAlO}_2\text{-}\gamma\text{-Al}_2\text{O}_3$  did not form  $m\text{-Al}_2\text{O}_3$  could not be explained clearly, two reasons could be given: (i) very intimate and uniform mixing of  $\text{NaAlO}_2$  and  $\gamma\text{-Al}_2\text{O}_3$  was not achieved on a microscopic level, and (ii)  $\beta''\text{-Al}_2\text{O}_3$  had the thermodynamic tendency to be formed more easily compared to  $m\text{-Al}_2\text{O}_3$ . The former reason is questionable because the  $m$  phase was formed in samples such as N-5A which are rich in  $\gamma\text{-Al}_2\text{O}_3$ . Concerning the latter, when there

is a possibility of the formation of two compounds, the compound with the lower activation energy of formation will be formed predominantly. In the present experiment,  $E_a$  for the formation of  $\beta''\text{-Al}_2\text{O}_3$  in N-2A (130–135 kcal/mole, Figs. 8 and 10) is higher than that for the formation of  $m\text{-Al}_2\text{O}_3$  in N-5A (55–60 kcal/mole, Figs. 8 and 12). Therefore, it seems to be difficult to accept the latter reason. However, the values of  $E_a$  mentioned above should not be compared from the same point of view because they are concerned with different samples with different compositions, and moreover, they are concerned chiefly with the activation energies for diffusion or growth and do not relate to the nucleation behavior of  $\beta''\text{-}$  or  $m\text{-Al}_2\text{O}_3$  since the present reactions have been assumed to be diffusion limited. Although the problem of nucleation and growth must be resolved in the future, the present authors lean toward the latter reason.

## 3. Transitions of $m\text{-Al}_2\text{O}_3$ to $\beta\text{-Al}_2\text{O}_3$

The activation energy,  $E_a$ , for the  $\beta\text{-Al}_2\text{O}_3$  formation in N-5A is about 95–100 kcal/mole, and  $E_a$  for the formation of  $\beta''\text{-Al}_2\text{O}_3$  in N-2A is about 130–135 kcal/mole. Thus,  $E_a$  for the formation of  $\beta\text{-Al}_2\text{O}_3$  is lower by about 35 kcal/mole than that for the formation of  $\beta''\text{-Al}_2\text{O}_3$ . The difference suggests a difference in the process of formation between  $\beta\text{-}$  and  $\beta''\text{-Al}_2\text{O}_3$  in the samples N-5A and N-2A. As mentioned above, the formation of  $\beta''\text{-Al}_2\text{O}_3$  in N-2A could not be explained well.

It is useful to note that the initiation line of the  $m\text{-Al}_2\text{O}_3$  formation in Fig. 2 is situated lower than that of the  $\beta''\text{-Al}_2\text{O}_3$  formation in Fig. 1.  $E_a$  for the  $m\text{-Al}_2\text{O}_3$  initiation or maximization in N-5A is 55–60 kcal/mole. The difference between  $E_a$  for the initiation of the  $\beta\text{-Al}_2\text{O}_3$  formation and that for the maximization of the  $m\text{-Al}_2\text{O}_3$  formation in N-5A is estimated to be about 40 kcal/mole, which is equal to the difference between  $E_a$

obtained from the curve in Fig. 10 and that calculated from the Jander plot. Concerning sample N-5A, it can be said from several values of  $E_a$  that (i) the value of 55–60 kcal/mole represents the activation energy for the formation of m- $\text{Al}_2\text{O}_3$ , (ii) the value of 35–40 kcal/mole signifies the transition enthalpy of m- $\text{Al}_2\text{O}_3$  to  $\beta$ - $\text{Al}_2\text{O}_3$ , and (iii) the sum of the two values corresponds to the activation energy of 95–100 kcal/mole for the formation of the  $\beta$  phase. The present experiments may confirm qualitatively geometrical speculation that only a minor structural rearrangement is required to convert mullite-like " $\lambda$ - $\text{Al}_2\text{O}_3$ " to  $\beta$ - $\text{Al}_2\text{O}_3$  (5).

### Summary

The solid state reactions in the system  $\text{NaAlO}_2$ - $\gamma$ - $\text{Al}_2\text{O}_3$  were studied kinetically. In the region of  $\text{NaAlO}_2$ -rich composition,  $\beta'$ - $\text{Al}_2\text{O}_3$  was formed. In the region of  $\gamma$ - $\text{Al}_2\text{O}_3$ -rich composition, mullite-type m- $\text{Al}_2\text{O}_3$  was formed primarily and it later transformed to  $\beta$ - $\text{Al}_2\text{O}_3$ . The mechanism of

m- $\text{Al}_2\text{O}_3$  formation was discussed referring to the mullite formation from  $\text{SiO}_2$  and  $\gamma$ - $\text{Al}_2\text{O}_3$ .

### References

1. R. C. DEVRIES AND W. L. ROTH, *J. Amer. Ceram. Soc.* **52**, 364 (1969).
2. J. LIEBERTZ, *Ber. Deut. Keram. Ges.* **49**, 288 (1972).
3. J. FALLY, C. LASNE, Y. LAZENNEC, Y. LECARS, AND P. MARGOTIN, *J. Electrochem. Soc.* **120**, 1296 (1973).
4. A. J. PERROTTA AND J. E. YOUNG, JR., *J. Amer. Ceram. Soc.* **57**, 405 (1974).
5. A. G. ELLIOT AND R. A. HUGGINS, *J. Amer. Ceram. Soc.* **58**, 497 (1975).
6. S. T. LUNDIN, *Geol. Foeren. Stockholm Foerh.* **80**, 458 (1958).
7. M. AVRAMI, *J. Chem. Phys.* **7**, 1103 (1939); **8**, 212 (1940); **9**, 177 (1941).
8. B. V. EROFEEV, *Dokl. Akad. Nauk SSSR* **52**, 511 (1946).
9. W. JANDER, *Z. Anorg. Chem.* **163**, 1 (1927).
10. A. M. GINSTLING AND B. I. BROUNSHTEIN, *J. Appl. Chem. USSR* **23**, 1327 (1950).
11. J. T. KUMMER, *Progr. Solid State Chem.* **7**, 141 (1972).
12. B. B. GHATE, D. P. H. HASSELMAN, AND R. M. SPRIGGS, *Ceram. Bull.* **52**, 670 (1973).